

# Effects of natural mutations in lecithin:cholesterol acyltransferase on the enzyme structure and activity

F. Peelman,\* J-L. Verschelde,† B. Vanloo,\* C. Ampe,† C. Labeur,\* J. Tavernier,†  
J. Vandekerckhove,† and M. Rosseneu<sup>1,\*</sup>

Laboratory for Lipoprotein Chemistry,\* and the Flanders Interuniversity Institute for Biotechnology,†  
Department of Biochemistry, Faculty of Medicine, Universiteit Gent, B-9000 Gent, Belgium

**Abstract** A molecular model was built for human lecithin:cholesterol acyltransferase (LCAT) based upon the structural homology between this enzyme and lipases (Peelman et al. 1998. *Prot. Sci.* 7: 585–597). We proposed that LCAT belongs to the  $\alpha/\beta$  hydrolase fold family, and that the central domain of LCAT consists of a mixed seven-stranded  $\beta$ -pleated sheet with four  $\alpha$ -helices and loops linking the  $\beta$ -strands. The catalytic triad of LCAT was identified as Asp345 and His377, as well as Ser181. This model is used here for the interpretation of the structural defects linked to the point mutations identified in LCAT, which cause either familial LCAT deficiency (FLD) or fish-eye disease (FED). We show that these mutations occur in separate domains of the 3D structure of the enzyme. Most mutations causing familial LCAT deficiency are either clustered in the vicinity of the catalytic triad or affect conserved structural elements in LCAT. Most mutations causing fish-eye disease are localized on the outer hydrophilic surface of the amphipathic helical segments. These mutations affect only minimally the overall structure of the enzyme, but are likely to impair the interaction of the enzyme with its co-factor and/or substrate.—Peelman, F., J-L. Verschelde, B. Vanloo, C. Ampe, C. Labeur, J. Tavernier, J. Vandekerckhove, and M. Rosseneu. Effects of natural mutations in lecithin:cholesterol acyltransferase on the enzyme structure and activity. *J. Lipid Res.* 1999. 40: 59–69.

**Supplementary key words** lecithin:cholesterol acyltransferase • mutants • enzymatic activity • structure • lipoproteins • reverse cholesterol transport

Lecithin:cholesterol acyltransferase (LCAT) is a key enzyme in lipoprotein metabolism, as it accounts for the synthesis of most of the plasma cholesteryl esters (1, 2). This enzyme catalyzes the transacylation of the *sn*-2 fatty acid of lecithin to the free 3- $\beta$  hydroxyl group of cholesterol, whereby lysolecithin and cholesteryl ester are formed. LCAT plays a major role in the maturation of lipoprotein particles by converting cholesterol into cholesteryl esters, which are incorporated into the core of the plasma lipoproteins. Lecithin:cholesterol acyltransferase is active on both low density (LDL) and high density lipoproteins (HDL),

corresponding to, respectively, the  $\beta$ - and  $\alpha$ -activity of LCAT (2). Cloning of the LCAT gene demonstrated that  $\alpha$ - and  $\beta$ -activity represent two functions of the same protein (3, 4).

Mutations in the LCAT gene underlie either familial LCAT deficiency (FLD) or fish-eye disease (FED) which are both inherited in an apparent autosomal recessive manner (5). FLD was first reported in 1967 (6). The probands of this Norwegian family had a virtual absence of LCAT activity in plasma, and reduced LCAT concentration and cholesteryl esters content. This disorder was characterized by HDL deficiency and abnormal triglyceride-rich VLDL and LDL. The major clinical findings were corneal opacification, anemia, proteinuria, and renal disease; similar clinical observations have been made in most of the patients identified more recently (7).

A second genetic disorder known as FED or partial LCAT deficiency was reported by Carlson and Philipson (8) in two families of Swedish origin. The only clinical manifestation in these patients was corneal opacification which increased with age. The patients had HDL deficiency and elevated triglyceride levels. As the cholesteryl ester content of HDL was strongly reduced whereas that of VLDL and LDL was normal, it was proposed that FED is caused by the lack of the LCAT  $\alpha$ -activity on HDL, while the  $\beta$ -activity on LDL is preserved (7, 9). Gene defects leading to either FLD or FED were recently reviewed by Kuivenhoven et al. (5), who listed these defects in four different classes. FLD is caused either by null or missense mutations: in Class 1 defects, null mutations cause total loss of catalytic activity and virtual absence of LCAT mass, while in Class 2 missense mutations are characterized by loss of activity and either normal, reduced, or absent LCAT mass. FLD is caused by missense mutations only; these mutations affect either LDL or LDL and HDL activity in Class 3 defects, while LCAT mass is reduced. In Class 4 defects, the

Abbreviations: HDL, high density lipoproteins; LDL, low density lipoproteins; VLDL, very low density lipoproteins; LCAT, lecithin:cholesterol acyltransferase; FLD, familial LCAT deficiency; FED, fish-eye disease.

<sup>1</sup>To whom correspondence should be addressed.

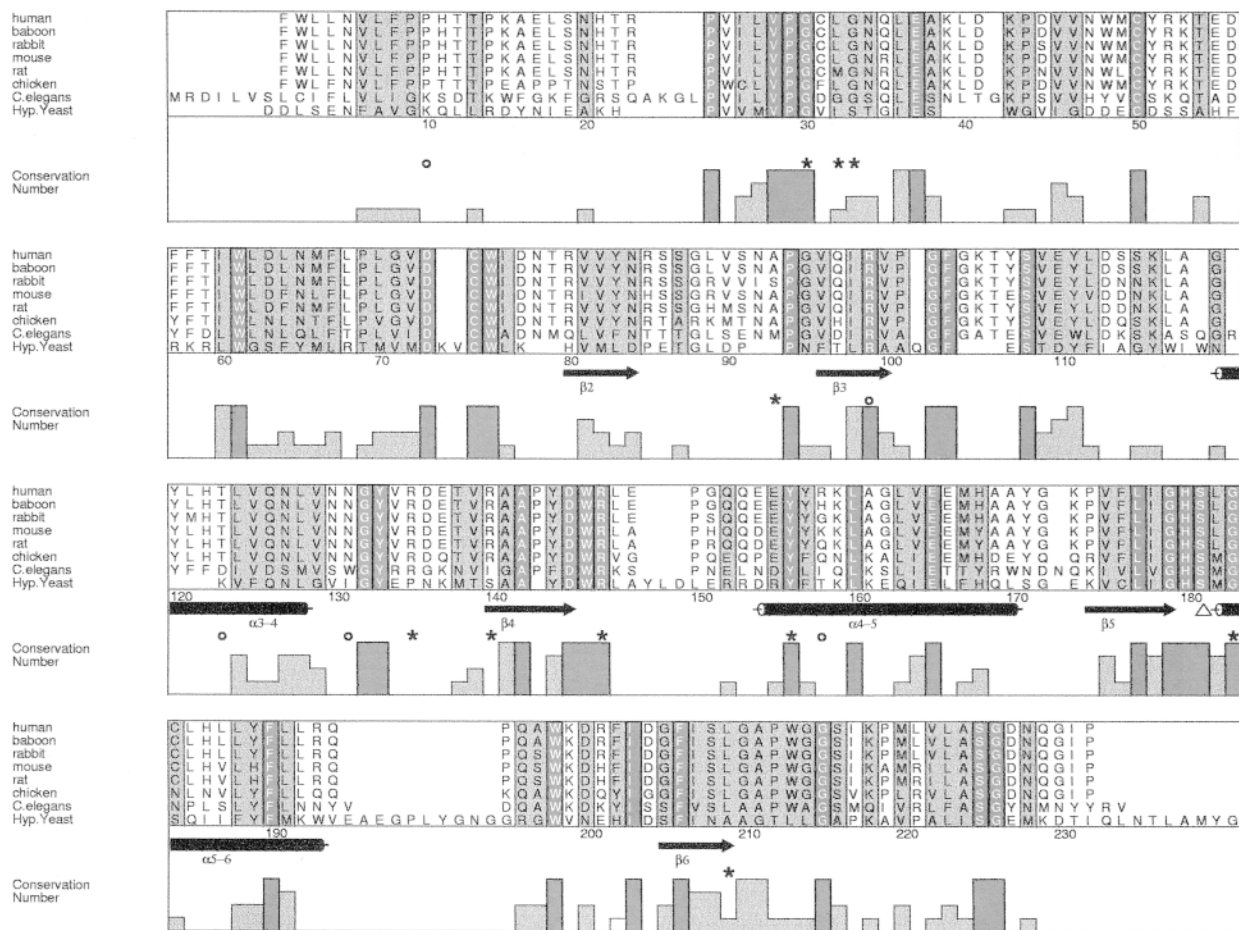


**Fig. 1.** CLUSTAL W alignment of the LCAT sequences of human, baboon, rabbit, mouse, rat, chicken, and *C.elegans* with residues 151–661 of the hypothetical 75.4 kD protein identified on chromosome XIV of *Saccharomyces cerevisiae* (18). Residue numbering corresponds to human LCAT. Identical residues are shown in reverse video mode; conserved residues are shaded. The bar plot under the alignment represents the conservation number calculated using the method of Livingstone and Barton (20). A value of 7 was taken as the cut-off for residue conservation, and values under this cut-off are not displayed. Previously proposed secondary structure elements (13) are drawn under the aligned sequences. Arrows are  $\beta$ -strand, cylinders are  $\alpha$ -helix. The active site residues are indicated by triangles. Residues affected in FLD are indicated with an asterisk (\*), residues affected in FED are indicated with a circle ( $\odot$ ) under the alignment.

missense mutations are associated with partial loss of activity against HDL only and reduced LCAT mass.

LCAT is a glycoprotein with an apparent molecular mass of 67 kDa that consists of 416 residues (3, 4) and 25% of the LCAT mass is carbohydrate, which is covalently linked to four N-glycosylation sites (N20, N84, N272, N384) and two O-glycosylation sites (T407 and S409) (10). The enzyme is expressed in the liver and secreted into the plasma compartment where it is primarily associated with HDL particles, containing the major activator for LCAT, apolipoprotein A-I (apoA-I) (2).

The tertiary structure of LCAT is unknown, but important functional residues of the enzyme were identified by chemical modification (11) and site-directed mutagenesis (12). We proposed that LCAT, like lipases, belongs to the  $\alpha/\beta$  hydrolase fold family, and that the central domain of LCAT consists of seven conserved  $\beta$ -strands connected by four  $\alpha$ -helices and separated by loops (13). A long excursion at residues 210–332 separates the N- and C-terminal domains of LCAT. In addition to the known S181 residue

(12), we identified D345 and H377 by site-directed mutagenesis as the catalytic residues of LCAT, together with F103 and L182 as the oxyanion hole residues. An interfacial recognition domain, involved in the enzyme–substrate interaction was also proposed at residues 50–74 of LCAT (13). A 3D model for human LCAT was obtained by molecular modeling, using human pancreatic and *Candida antarctica* lipases as templates (13). In this model we could only include those residues with enough structural homology to the lipases, i.e., from residues 73–210 for the N-terminal domain and residues 332–393 for the C-terminal domain. The long excursion at residues 211–332 was not included due to lack of an appropriate template (13).

The expanding list of pathological point mutations in the LCAT gene leading to the development of either FLD or FED (see Table 1) is in need of structural interpretation. In the absence of an X-ray structure, we used the 3D model proposed for LCAT (13) to provide a structural interpretation of the effects of 18 different point mutations on the enzymatic function. The location

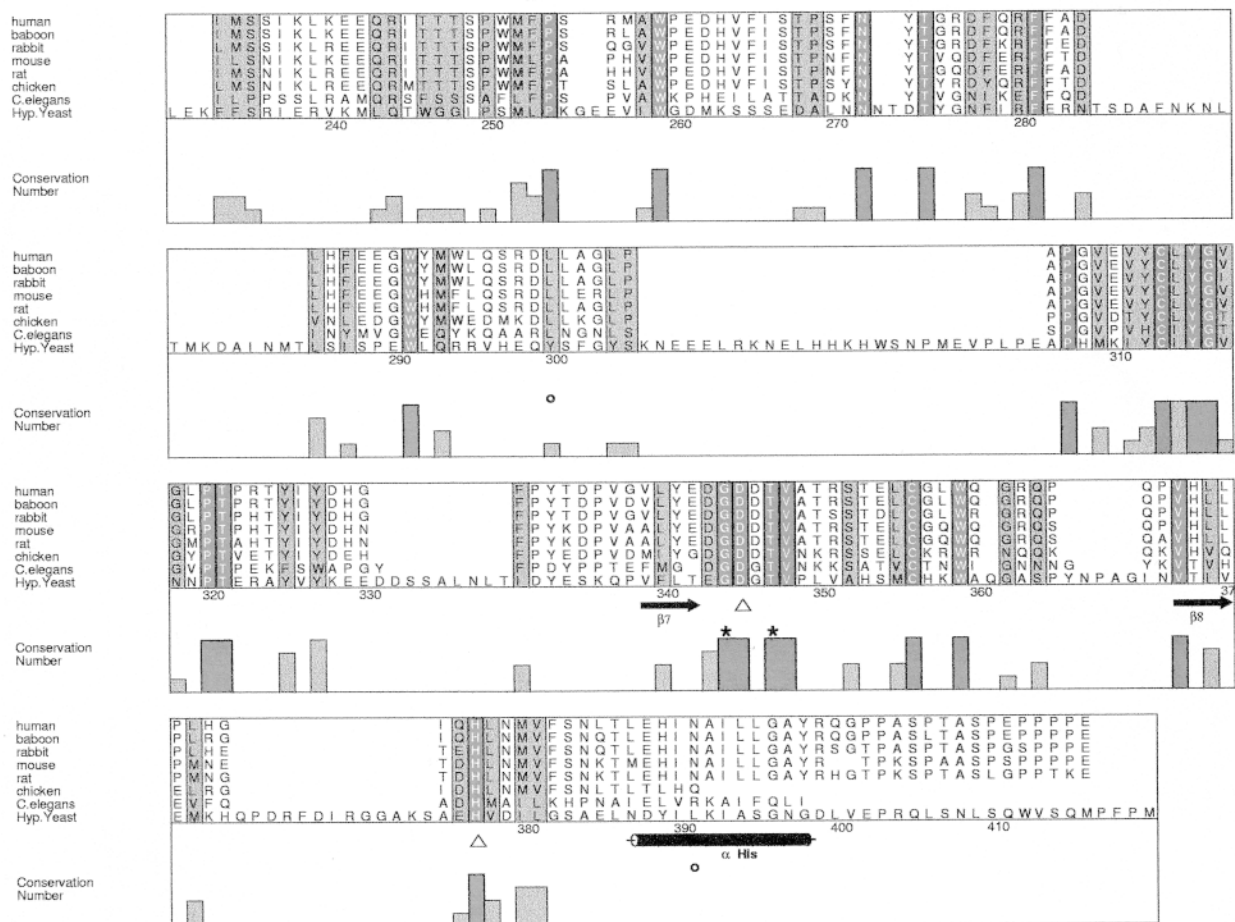


Fig. 1. (continued)

of different natural mutations had previously been used to check the validity of the model (13). This analysis is restricted to mutations occurring in the structurally conserved domains of LCAT, as the loops are highly variable elements in the lipase family that could not be modeled with sufficient confidence (13). These mutations include 13 missense mutations causing FLD, which belong to Class 2 of LCAT gene defects according to Kuivenhoven et al. (5), two Class 3 and one Class 4 mutations causing FED, and two mutations causing FED (14–16) which have not been classified yet. The effect of these point mutations on the enzyme structure provides a rationale for the reported deficiencies in the enzymatic activity of the different mutants.

## MATERIALS AND METHODS

The working model for human LCAT was built using the HOMOLOGY software (Biosym, San Diego, CA). Different naturally occurring mutations that have been reported were modeled using the same program. Side chains of the mutated residues were placed in their most favorable rotamer position. The sequences of human, baboon, rabbit, mouse, rat, chicken, *Caenorhabditis elegans* LCAT (17) and that of the hypothetical 75.4 kD *Saccharomyces cerevisiae* protein (18) were aligned using the CLUSTAL W

program (19), available at: <http://www2.ebi.ac.uk/clustalw>. Residue conservation number was calculated according to Livingstone and Barton (20) ([http://barton.ebi.ac.uk/servers/amas\\_server.html](http://barton.ebi.ac.uk/servers/amas_server.html)) and plotted using the Alscript software (21).

## RESULTS AND DISCUSSION

### Conserved structural elements in LCAT

The aligned sequences of human, baboon, rabbit, mouse, rat, chicken, and *C. elegans* LCAT, together with the sequence of the hypothetical 75.4 kD *S. cerevisiae* protein homologous to human LCAT, are shown in Fig. 1. The structural elements identified by threading (13) are shown in the same figure, as well as the sequence homology profile between species, calculated as described under Materials and Methods. The central domain of LCAT consists of a mixed 7-stranded  $\beta$ -pleated sheet, with four helices and loops linking the strands, in a way characteristic for this family of  $\alpha/\beta$  hydrolases (22). The sequence homology profile in Fig. 1 demonstrates that the most highly conserved elements in the eight sequences coincide with the strands of the central  $\beta$ -pleated sheet, in agreement with the observation that the architectural core of a protein is more conserved during evolution than any of the

peripheral elements, especially the loops (22). Other conserved elements in LCAT include helix  $\alpha$ 4-5 at residues 154–171 and the C-terminal end of helix  $\alpha$ 3-4 at residues 125–130. The best conserved residues are on the hydrophobic face of this amphipathic helix. Helix  $\alpha$ 3-4 packs against the central  $\beta$ -sheet, together with the C-terminal helix  $\alpha$ -His. The loop between  $\beta$ 3 and  $\alpha$ 3-4 at residues 102–115, corresponds to loop A in pancreatic and hepatic lipases (23, 24). It has significant conservation level (Fig. 1), and is possibly involved in the changes from a closed to an open configuration of the enzyme. Other conserved residues include the sequences around the catalytic residues S181, D345, and H377 and the oxyanion hole residues F103 and L182 of human LCAT (13) (Fig. 1). The cysteine bridges at residues 50–74 and 313–356 are also strictly conserved.

### Variable structural elements in LCAT

Among the helices connecting the  $\beta$ -strands, helices  $\alpha$ 3-4,  $\alpha$ 5-6, and  $\alpha$ -His are more variable than helix  $\alpha$ 4-5 (Fig. 1). The loop connecting strands  $\beta$ 2 to  $\beta$ 3 at residues 85–96 and that connecting strand  $\beta$ 4 to helix  $\alpha$ 4-5 at residues 147–153 are highly variable among species. The latter loop is possibly involved in binding of the *sn*-2-acyl chain, as the E149A mutation was shown by Wang et al. (25) to alter the phospholipid acyl chain specificity of LCAT. The insertions in the sequence of the hypothetical 75.4 kD *S. cerevisiae* protein, when aligned with LCAT of different species, occur mostly in loops and in structural elements that are not part of the typical  $\alpha/\beta$ -hydrolase fold. As a whole, the N-terminal part of LCAT (residues 1–220) is better conserved than the C-terminal domain (Fig. 1), due to the variability of the long excursion at residues 211–323 (13). The length of the C-terminal helix  $\alpha$ -His is variable among LCAT species (Fig. 1). This helix is truncated in chicken and *C. elegans* LCAT and in the *S. cerevisiae* protein, and it has a 2-residue deletion in mouse LCAT (Fig. 1). Human LCAT mutants truncated beyond G401 (26) showed that the C-terminal residues are not critical for enzymatic activity.

### Structural effects of point mutations in the LCAT gene: point mutations associated with FLD

**FLD point mutations in the vicinity of the catalytic triad. G183S.** This mutation was detected in two Canadian brothers with corneal opacity (27). The probands had no detectable LCAT activity in plasma (Table 1). G183 is part of the consensus sequence GX SXG, which is the signature of the  $\alpha/\beta$  hydrolase family (22). The GX SXG motif forms a type  $\gamma$  turn with the active site serine G183 in an unfavourable  $\epsilon$  conformation. This particular conformation brings  $\alpha$ 5-6 very close to  $\beta$  strands 4, 5, and 6. Residues G179 and G183 come very close to each other and the serine side chain at position 183 causes severe steric hindrance with neighbors V100, P101, and G179 (Fig. 2A) and impairs proper folding of the enzyme (27).

**L209P.** This mutation was described in a French patient presenting the typical FLD phenotype (28–30). Transfection of the mutant enzyme into BHK (31) and

into Cos-6 cells (32) yielded no detectable amount of protein in the cellular media (Table 1), while transfection into Cos-1 cells produced a small amount of inactive enzyme (31). This mutation occurs in strand  $\beta$ 6 of LCAT, one of the highly conserved structural elements of the central  $\beta$ -sheet (Fig. 1). The L209P substitution probably impairs the proper folding of the mutant LCAT, as the insertion of a proline residue disturbs the regular structure of strand  $\beta$ 6 and causes steric hindrance between P209 and G179 (Fig. 2B). Alternatively, due to the close proximity of the C-terminal end of strand  $\beta$ 6 to the catalytic residues S181-D345-H377, the L209P substitution perturbs the proper orientation of these residues (Fig. 2B).

**G344S, T347M.** These two mutations are associated with FLD in two separate probands (33, 34). The G344S mutation was identified in a Japanese patient who had 10% of normal LCAT mass and no measurable activity (34) (Table 1). Both mutations occur in the double-turn around the active site D345 after strand  $\beta$ 7 (13) (Fig. 1). The G344S mutation is contiguous to the active site D345, and the particular conformation of G344 is probably not compatible with its substitution by a serine residue (Fig. 1, Fig. 2C). This mutation therefore impairs the right orientation of D345 in the active site cavity, so that the enzyme cannot fold properly. Transfection of this mutant into Cos-1 cells did not lead to the expression of any detectable mass or activity (33) (Table 1).

The T347M mutation occurs as a compound heterozygote mutation in a patient who had 50% normal plasma LCAT mass but no activity (34). The effect of the T347M mutation is less severe, as this substitution causes no steric hindrance with neighbors (Fig. 2C), and it only decreases the accessibility of the substrate to the cavity around the catalytic triad. The enzyme structure is less perturbed, and in vitro expression showed that the protein was secreted at about half of normal levels and had 3–10% activity compared to wild-type LCAT (Table 1) (31, 32, 35).

**G30S, L32P, G33R.** These mutations all result in an inactive enzyme and lead to the typical phenotype of the LCAT deficiency syndrome (27, 36, 37). In vitro expression of the G30S and L32P mutants showed that the mutant protein is still secreted, but that it is inactive (Table 1) (32, 36). The mutations at positions 30, 32, and 33 of LCAT either cause steric hindrance (G30S), introduce an extra charged residue (G33R), or modify the secondary structure of the segment (L32P). This highly conserved N-terminal region of LCAT (Fig. 1) seems critical for the full activity of the enzyme, probably due to the vicinity of C31 and C184, which come in close spatial proximity to the active site nucleophile S181 in mammalian LCAT species (38). The vicinity of these two cysteines in the spatial configuration of LCAT (38), is reflected by both the conservation of the two cysteines in mammalian LCAT and by their changes to different residues in other LCAT species (Fig. 1).

**FLD point mutations in conserved structural elements of LCAT. R147W.** This mutation, described by Taramelli et al. (39), affects a male proband and leads to complete loss of LCAT activity in plasma (Table 1). When the recombinant protein was expressed in HEK293, Cos-1, or Cos-6 cells,

TABLE 1. Point mutations causing familial LCAT deficiency: LCAT mass,  $\alpha$ -LCAT activity and CER in plasma of patients with FLD; LCAT mass and specific activity of in vitro expressed mutants on r-HDL and on LDL

Mutation		LCAT Mass and Activity in Plasma of FLD Patients				LCAT Mass and Activities in In Vitro Expression				
		LCAT Mass <sup>a</sup>	CER <sup>a,b</sup>	$\alpha$ -LCAT <sup>a,c</sup>	Ref.	Cellular Expression System	LCAT Mass <sup>d</sup>	$\alpha$ -LCAT <sup>c</sup> Specific Activity <sup>d</sup>	Specific Activity on LDL <sup>d</sup>	Ref.
			<i>% of control</i>				<i>% of wild-type</i>			
G30S	Homozygous	47	12–36	0	36	COS-7	92	0		36
L32P	Compound Heterozygous (+T321M)		<10		27	COS-6	66	<1	2	32
G33R	Compound Heterozygous (+33bp ins.)		4	5	37					
A93T	Compound Homozygous (+R158C)		0	3	28	COS-6 COS-1	75 88	25 7	4	32 31,42
R135W	Compound Homozygous (+bp ins.)	0	0	0	28	COS-6 COS-1 BHK	20 145	2 0 0.1	5 0.8	32 31 31
R135Q <sup>e</sup>	Compound Heterozygous (+P10Q.)	64	83	8	43	BHK		1	4	43
R140H	Homozygous			0	44	COS-7		0		44
R147W	Homozygous	60	0	0	39	COS-6 HEK-293 COS-1	0 0 0			32 35 39
Y156N	Compound Heterozygous (+Y83stop)	3.5	0	1.5	40	HEK-293	6	32		35,40
G183S	Compound Heterozygous (+frameshift)	4		2	27					
L209P	Homozygous	3	0 8	0 15	28 29,30	COS-6 COS-1 BHK	0 24	1 0	0	32 31 31
G344S	Homozygous	9	1	0	33	COS-1	<10	0		33
T347M <sup>e</sup>	Compound Heterozygous (+T123I)	50–80	50–80	0.9	34	COS-6 HEK-293 COS-1 BHK	60 43 101	11 <10 3 3	12 8	32 35 31 31

<sup>a</sup>Values for LCAT mass and activity in the FLD patients are expressed as % of normal values in control subjects.

<sup>b</sup>CER:cholesterol esterification rate (28).

<sup>c</sup> $\alpha$ -LCAT activity was measured on r-HDL or by proteoliposome assay.

<sup>d</sup>LCAT mass and specific activities for in vitro expression are expressed as % of the values for expressed wild-type LCAT.

<sup>e</sup>The R135Q and T347M mutations were found in compound heterozygous FED patients, but in vitro expression led to a nearly complete loss of LCAT activity. Kuivenhoven et al. (5) therefore classified these mutations as Class 2 LCAT gene defects.

neither mass nor activity were detectable, although up to 60% of normal LCAT mass was detected in the patient's plasma (Table 1) (32, 35, 39). Modeling of this region shows that, in analogy with pancreatic lipase (23, 24), R147 lies at the extremity of strand  $\beta$ 4 at 3.2 Å of D145, suggesting that it makes a salt bridge with this acid residue (Fig. 3A). D145 lies in turn at 3.4 Å of R80, with which it might form another salt bridge. Both R147 and D145 are strictly conserved in all LCAT species (Fig. 1) The R147W mutation substitutes a bulky tryptophan for the arginine at this position and it inhibits the formation of the first salt bridge (Fig. 3A). This destabilizes the structure of the LCAT protein.

*Y156N*. This mutation is accompanied by the clinical

FLD phenotype in a 54-y male patient, who was a compound heterozygote for this and the Y83stop mutation (40). Both LCAT mass and activity were severely reduced in plasma (Table 1). Expression of this mutant in HEK293 cells yielded low mass (6%) but 32% activity for the mutant, compared to WT LCAT (35, 40). This mutation introduces a hydrophilic residue in the conserved hydrophobic face of the amphipathic helix  $\alpha$ 4-5, thereby decreasing the hydrophobic moment of this helix (Fig. 1, Fig. 3B), and the lipid-binding capacity of the corresponding synthetic peptide (41). Moreover, as the hydrophobic face of helix  $\alpha$ 4-5 packs against the hydrophobic side of the central  $\beta$ -sheet, Y156 comes close to Y144 and W146 of strand  $\beta$ 4 (Fig. 3B) (13). The Y156N mutation thus per-

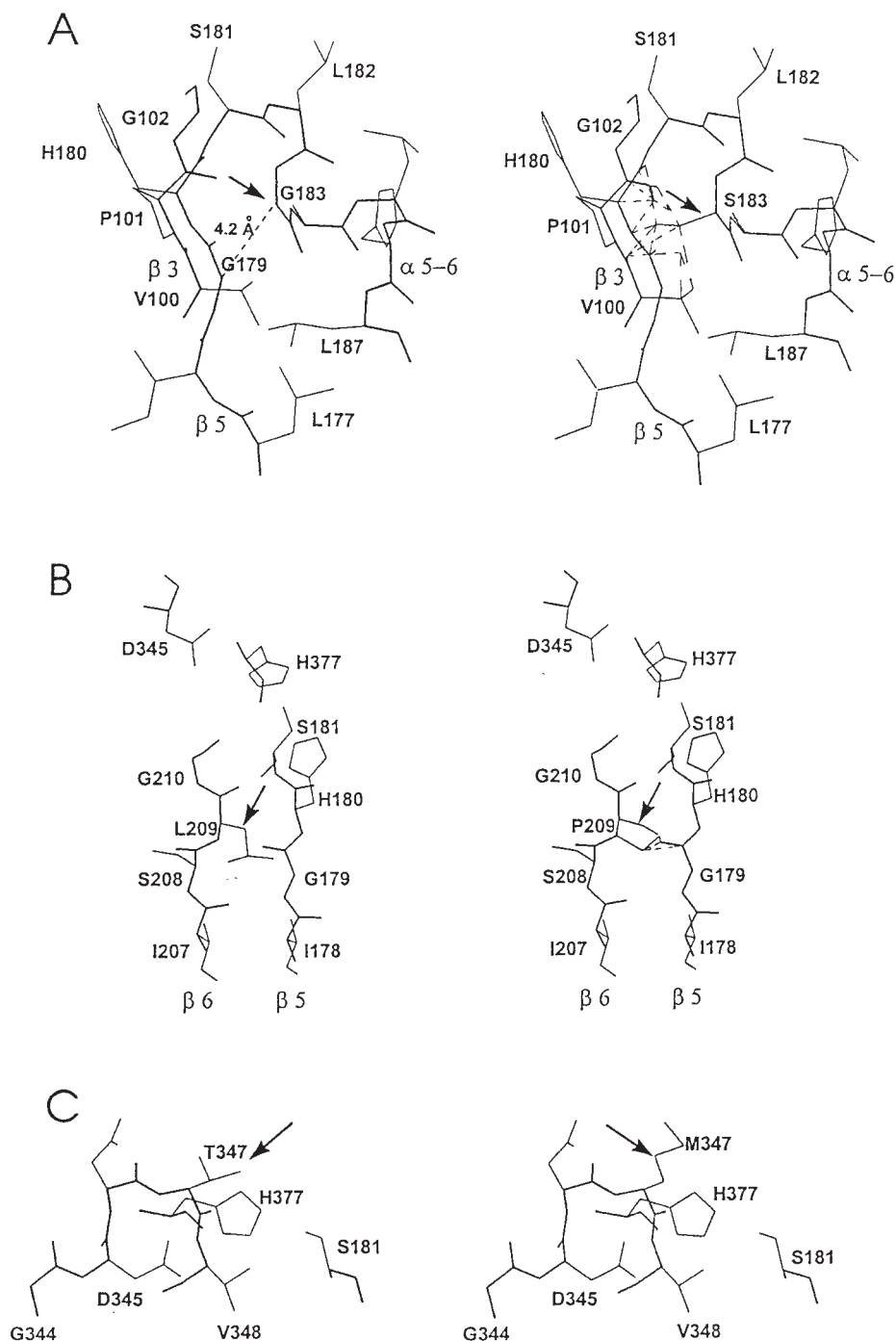


**Fig. 2.** Structure comparison of WT LCAT with FLD mutants occurring in the vicinity of the catalytic triad. This figure compares the structure of wild-type LCAT (left) to that of the mutants (right), as modeled by the HOMOLGY (Biosym) program. Mutated residues are indicated by an arrow. Steric hindrance is shown by dotted lines. A: G183S mutation. This figure represents residues in strand  $\beta 3$  (V100–G102), strand  $\beta 5$  (L177–H180) and in helix  $\alpha 5-6$  (L182–L187) in human LCAT. The GHSLG motif at residues G179–G183 forms a sharp  $\gamma$ -like turn bringing the  $C\alpha$  atoms of G179 and G183 at 4.2 Å (left). The G183S mutation (right) causes steric hindrance of the side-chain of S183 with V100 and P101 in strand  $\beta 3$  and with G179 and H180 in  $\beta 5$ , N-terminal of the active site residue S181. B: L209P mutation. This diagram shows part of strand  $\beta 5$  at residues I178–H180 and  $\beta 6$  at I207–G210, together with the active site triad, in WT LCAT (left). The L209P mutation (right) causes steric hindrance between P209 and G179 in strand  $\beta 5$  and impairs regular  $\beta$ -sheet hydrogen bonding between these two residues (right). C: T347M mutation. This diagram presents the double-turn motif around the active site D345 together with the active site triad (left). The T347M mutation (right) does not cause steric hindrance with neighbors, however the long Met side-chain restricts accessibility to the active site cavity.

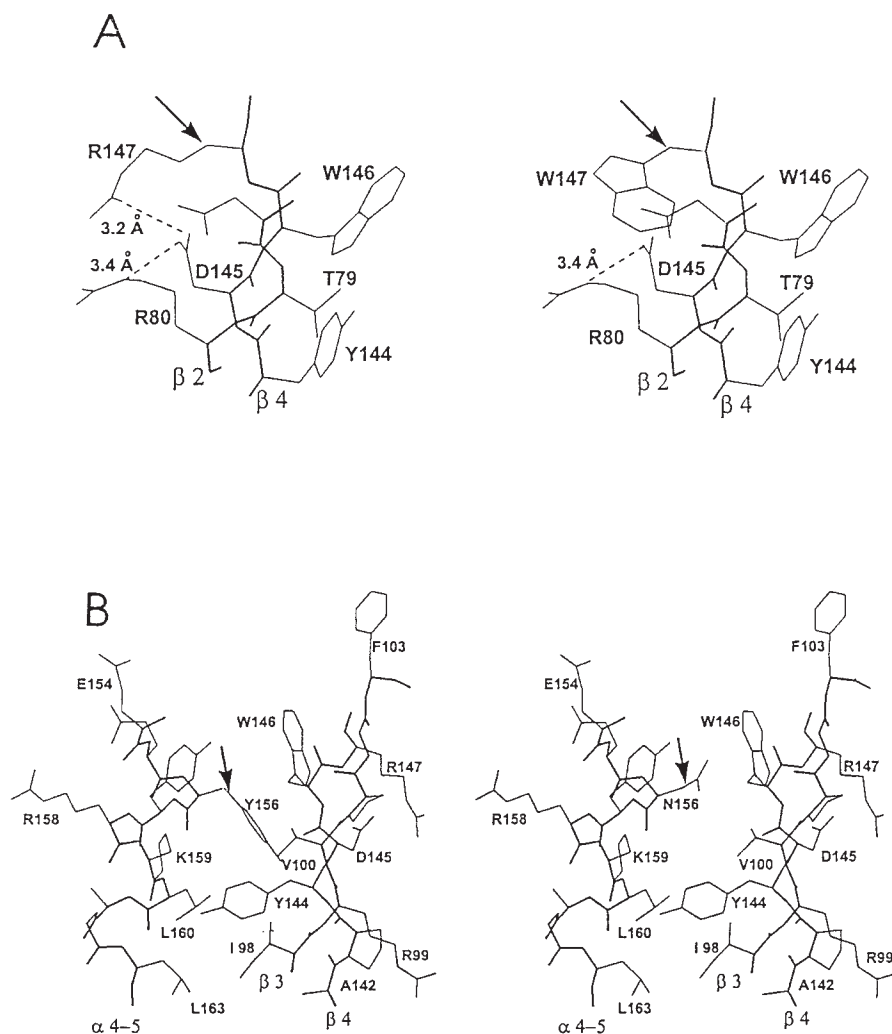


**Fig. 3.** Structure comparison of WT LCAT with FLD mutants occurring in conserved structural elements in LCAT. This figure compares the structure of wild-type LCAT (left) to that of the mutants (right), as modeled by the HOMOLGY (Biosym) program. Mutated residues are indicated by an arrow. A: R147W mutation. This figure shows residues N78–R80 in strand  $\beta 2$  and Y144–R147 in strand  $\beta 4$  of WT LCAT, illustrating the salt bridges of D145 with R80 and R147 (left). The R147W mutation impairs salt bridge formation between D145 and W147 (right). B: Y156N mutation. This figure shows part of strand  $\beta 3$  at residues I98–F103, strand  $\beta 4$  at A142–R147 and helix  $\alpha 4-5$  at E154–L163. Clustering of hydrophobic residues Y156, L160, and L163 on the hydrophobic side of helix  $\alpha 4-5$  against residues I98, V100 of strand  $\beta 3$  and Y144 and W146 of  $\beta 4$  (left). The Y156N mutation impairs hydrophobic interactions of this residue with V100, Y144, and W146 (right).

turbs the hydrophobic cluster of aromatic residues and probably decreases the stability of the  $\alpha/\beta$  hydrolase fold of LCAT.

**FLD point mutations occurring in variable structural elements of LCAT. A93T.** This mutation was detected in a Danish male patient (28) with reduced plasma LCAT activity on HDL and no detectable activity on LDL. The patient was a compound heterozygote for the A93T and R158C mutations (28). In vitro expression showed that the A93T mutant enzyme is secreted but its activity on both HDL and LDL is decreased (Table 1) (31, 32, 42).

**R135W, R135Q, R140H.** The first mutation was identified in two probands in a Canadian family of Italian-Dutch descent who were compound heterozygotes for a frame-shift mutation after residue 376 (28). The probands presented with the typical clinical features of familial LCAT

deficiency, including corneal opacity, anemia, and kidney disease. They had extremely low HDL levels, no detectable LCAT mass or activity. The R135Q mutation was found in a 53-y Dutch patient with angina pectoris and corneal opacity (43). The patient had low HDL levels and mildly elevated triglycerides. The LCAT mass was 80% and the activity around 10% normal. This patient appeared to be a compound heterozygote for the P10Q and R135Q mutations. When the latter mutant was expressed in BHK cells, it had no activity on either HDL or LDL (43). The R140H substitution was diagnosed in a 46y Austrian patient and in two of his siblings, who showed the typical clinical symptoms of FLD (44). No LCAT activity was detectable in the proband's plasma. When the mutant was transfected into Cos-7 cells, no LCAT activity was measurable in the medium (44).

Residue A93 is localized in the loop between strand  $\beta$ 2 and  $\beta$ 3, while R135 and R140 are found in the loop connecting helix  $\alpha$ 3-4 and strand  $\beta$ 4 (Fig. 1). While the other FLD mutants described in this paper affect amino acids that are conserved (Fig. 1), these three residues are variable, as they lie in surface loops. Although modeling of these variable loops using the HOMOLOGY program was not informative, we observed that, in the 3D model proposed for LCAT (13), the loop between strands  $\beta$ 2 and  $\beta$ 3 and that between helix  $\alpha$ 3-4 and strand  $\beta$ 4 come close to each other. These four mutants might therefore have a common effect on substrate binding as they affect LCAT activity on both HDL and LDL.

#### Point mutations associated with FED

**R99C.** This mutation was detected in a Spanish patient presenting the FED phenotype (14). Expression of the mutant in Cos-7 cells showed decreased activity on both r-HDL and on LDL (Table 2). The R99 residue lies on the hydrophilic side of strand  $\beta$ 3 in the core of the LCAT protein and is highly conserved (Fig. 1) (13). As R99 points towards helices  $\alpha$ 3-4 and  $\alpha$ -His (Fig. 4), this orientation brings it close to residues T123, N131, and N391 which are affected in FED mutants.

**T123I.** This mutation was the first to be associated with the FED phenotype, and the study of the proband helped define and differentiate between the  $\alpha$ - and  $\beta$ -activity of LCAT (45). This homozygous patient and heterozygous carriers of this mutation (34, 46) lost LCAT activity on HDL, but retained a high cholesterol esterification rate and activity on LDL (Table 2). In vitro expression of the T123I mutant LCAT confirmed a specific reduction of  $\alpha$ -LCAT activity (Table 2) (31, 32, 35, 47). We introduced an

alanine at this position and this mutant, expressed in Cos-1 cells, had normal mass and activity on LDL but lost its activity on HDL (F. Peelman and J. Tavernier, unpublished results). The results obtained by the expression of the T123I and T123A mutants thus suggest that the effect of the T123I mutation originates from the loss of the threonine side chain, in the hydrophilic side of helix  $\alpha$ 3-4, rather than from its substitution by a bulky hydrophobic isoleucine (Fig. 4).

**N131D.** This mutation was identified in four siblings with corneal opacification, who were homozygous for this mutation (48). The probands had reduced LCAT mass and activity as measured in a proteoliposome assay (Table 2). Stable expression of this mutant in BHK cells showed 4% residual activity on HDL and 25% on LDL (48) (Table 2). This mutation occurs also on the hydrophilic surface of helix  $\alpha$ 3-4 (Fig. 4), but it is more conservative than the T123I mutation.

**R158C.** Funke et al. (28) detected this mutation together with the A93T mutation (see above) in a patient with LCAT deficiency. Based upon in vitro expression experiments, Hill, Wang, and Pritchard (42) concluded that the A93T mutation was the defect underlying the disease, and that R158C was a co-inherited polymorphism (Table 2). However, the R158C mutation was later shown to cause FED (15, 16). Expression of the R158C mutation in Cos cells (32, 42) and in HEK293 cells (16, 35), suggests that this mutant lost part of its  $\alpha$ -LCAT activity, while its activity is retained on LDL (Table 2). R158 lies on the hydrophilic face of the  $\alpha$ 4-5 helix and points towards the solvent in the wild-type enzyme (Fig. 3B). Results obtained with the corresponding variant peptide at residues 154–171 suggest that lipid binding is decreased, probably due to the intro-

TABLE 2. Point mutations causing fish-eye disease: LCAT mass,  $\alpha$ -LCAT activity, and CER in plasma of patients with FED; LCAT mass and specific activity of in vitro expressed mutants on r-HDL and on LDL

Mutation		LCAT Mass and Activities in Plasma of FED Patients <sup>a</sup>				LCAT Mass and Activities in In Vitro Expression <sup>f</sup>				Ref.
		LCAT Mass <sup>a</sup>	CER <sup>a,b</sup>	$\alpha$ -LCAT <sup>a,c</sup>	Ref.	Cellular Expression System	LCAT Mass <sup>d</sup>	$\alpha$ -LCAT <sup>e</sup> Specific Activity <sup>d</sup>	Specific Activity on LDL <sup>d</sup>	
		<i>% of control</i>				<i>% of wild-type</i>				
R99C	Homozygous	50	45	25	14	COS-6	48	7	7	14
T123I	Homozygous	47–51	41–72	2–3	45	COS-6	84	8	143	32
						HEK-293	90	0–10		35
						COS-1	42	0.2	87	31,47
						BHK		31	104	31
N131D	Homozygous	29–36	50–87	5–10	48	BHK		4	25	48
R158C	Homozygous		19	6.5	16	COS-6	28	54	117	32
			16	37	15	COS-1	75	86		42
						HEK-293	35	70	100	16
						HEK-293	45	32		35
N391S	Compound Heterozygous (+M252K)	20–40	20	2–8	49	COS-1	92	15		31
								18	53	31

<sup>a</sup>Values for LCAT mass and activity in the FED patients are expressed as % of normal values in control subjects.

<sup>b</sup>CER:cholesterol esterification rate (28).

<sup>c</sup> $\alpha$ -LCAT activity was measured on r-HDL or by proteoliposome assay.

<sup>d</sup>LCAT mass and specific activities for in vitro expression are expressed as % of the values for expressed wild-type LCAT.



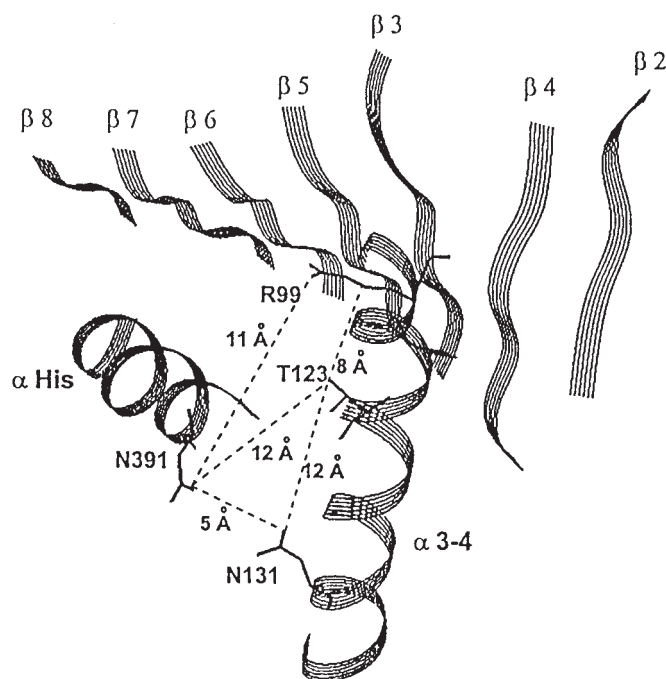


**Fig. 4.** Ribbon representation of helices  $\alpha$  3-4 and  $\alpha$ -His, packing against the central  $\beta$ -sheet in LCAT, showing residues involved in fish eye disease mutations. Residues T123, N131, and N391 lie on the outer surface of the amphipathic helices  $\alpha$ 3-4 and  $\alpha$ -His. R99 is part of strand  $\beta$ 3 and its side-chain lies close to  $\alpha$ 3-4.

duction of a cysteine in the hydrophilic face of the helix (41). The R158C substitution is less detrimental for the 3D structure of this mutant enzyme, but the solvent-exposed cysteine might be susceptible to oxidation.

**N391S.** The carriers of this mutation were compound heterozygotes for the N391S and the M252K mutations (49). When the mutants were expressed separately, the N391S mutant had 18% activity on HDL and 53% on LDL (31) (Table 2). The M252K mutant lost activity on both substrates, in agreement with a FLD pattern (50). The N391S mutation occurs at the C-terminal end of the  $\alpha$ -His helix (13) (Fig. 1). As this asparagine residue lies on the hydrophilic side of the  $\alpha$ -His helix, where it points towards helix  $\alpha$ 3-4, the N-S substitution at this position has only limited effect on the enzyme conformation (Fig. 4).

In the 3D model proposed for LCAT, T123, N131, and N391 lie on the surface of the protein, about 13 Å of each other (Fig. 4). This might constitute the primary domain of interaction between LCAT and its co-factor apoA-I, as the mutants lose more activity on r-HDL than on LDL.

## CONCLUSION

In this paper we correlate the structural and functional effects of point mutations in LCAT detected in either FLD or FED patients, using the 3D model proposed for the enzyme. Although there is no definitive proof for this model, as LCAT has not been crystallized yet, the analysis of the structural modifications caused by these point mutations

provides a link between the altered structure and impaired function of the enzyme. Our data show that most of the FLD mutants occur at positions that are strictly conserved among all LCAT species, including residues 30, 33, 147, 156, 183, 209, 344, and 347. On the contrary, sequence conservation is less strict for the FED mutants, as they occur at positions (residues 123, 131, 158, 391), that are not conserved in the most divergent species such as chicken and *C. elegans* LCAT. This suggests that, in agreement with the proposed conformation for these residues, missense mutations at these positions are less critical for the 3D structure of the enzyme and only partially affect its activity. The reported differences between phenotypes corresponding to either Class 3 mutations N131D and N391S or Class 4 mutation T123I (5) might be related to the structural differences between these residues. While they all lie on the surface and point towards the outside of the protein, T123 is closer to the catalytic triad in the 3D structure, accounting for the more severe phenotype associated with its mutation. This analysis further suggests that the clustering of the FLD and FED mutants in different parts of the LCAT 3D structure might account for the different phenotypes. FLD mutants G183S, L209P, G344S, T347M, and probably G30S, L32P, and G33R are in the vicinity of the catalytic triad in the 3D structure. The L209P and G183S mutants cause severe steric hindrance and impair proper folding, resulting in reduced LCAT mass. The Y156N mutation replaces a tyrosine in the hydrophobic interior of the enzyme with a hydrophilic residue, while the R147W mutation removes a possible conserved salt bridge.

In contrast to the FLD mutants, four of the five FED mutants that were modeled are on the protein surface on the hydrophilic face of the helical segments and therefore more accessible to solvent and substrate. Only the R99C mutant lies in the core of the enzyme. Among the mutations associated with FED, the P10Q (40), P10L (8, 51), T123I, N391S, N131D, R158C mutants are expressed at a significant level and lose more activity on HDL than on LDL (5). T123 and N131 lie on the hydrophilic surface of helix  $\alpha$ 3-4. In vitro expression of the T123I and N131D mutant LCAT, as well as the activity in the plasma of FED patients, shows that the  $\alpha$ -activity is more affected than the  $\beta$ -activity, suggesting that helix  $\alpha$ 3-4 is involved in the interaction of LCAT with HDL. As the activity of the R99C and  $\Delta$ L300 (52) FED mutants, is equally decreased on both substrates (Table 2), these results taken together suggest that the FED phenotype can originate from different defects, affecting the enzymatic activity on either one or both lipoprotein substrates. As described for mutants of lipoprotein and hepatic lipases (53), the screening procedure for natural mutants preferably selects those associated with either loss of mass or activity leading to lipoprotein abnormalities and to dyslipoproteinemia. Those mutations are likely to significantly affect the enzyme folding and stability. The differentiation between FLD and FED pathologies provides a new way for detection of less severe mutations, as described above. The type of analysis carried out in this paper is therefore helpful to relate the pathology of the

mutations and the structure of the LCAT enzyme, which profoundly affects lipoprotein metabolism. **PLM**

This work was supported by FWO grants 36004497 and G006196. C. A. is a Research Associate of the FWO-Vlaanderen. F. P. is a recipient of an IWT Doctoral Fellowship.

Manuscript received 8 May 1998 and in revised form 22 August 1998.

## REFERENCES

1. Glomset, J. A. 1962. The mechanism of the plasma cholesterol esterification reaction : plasma fatty acid transferase. *Biochim. Biophys. Acta.* **65**: 128-135.
2. Jonas, A. 1991. Lecithin:cholesterol acyltransferase in the metabolism of high-density lipoproteins. *Biochim. Biophys. Acta.* **1084**: 205-220.
3. McLean, J., C. Fielding, D. Drayna, H. Dieplinger, B. Braer, W. Kohr, W. Henzel, and R. Lawn. 1986. Cloning and expression of human lecithin:cholesterol acyltransferase cDNA. *Proc. Natl. Acad. Sci. USA.* **83**: 2335-2339.
4. McLean, J., K. Wion, W. Drayna, C. Fielding, and R. Lawn. 1986. Human lecithin:cholesterol acyltransferase gene: complete gene sequence and sites of expression. *Nucleic Acids Res.* **14**: 9397-9406.
5. Kuivenhoven, J. A., H. Pritchard, J. Hill, J. Frohlich, G. Assmann, and J. Kastelein. 1997. The molecular pathology of lecithin:cholesterol acyltransferase (LCAT) deficiency syndromes. *J. Lipid Res.* **38**: 191-205.
6. Norum, K. R., and E. Gjone. 1967. Familial plasma lecithin:cholesterol acyltransferase deficiency. Biochemical study of a new inborn error of metabolism. *Scand. J. Clin. Lab. Invest.* **20**: 231-243.
7. Glomset, J. A., G. Assmann, E. Gjone, and K. R. Norum. 1995. Lecithin:cholesterol acyltransferase deficiency and fish-eye disease. In *The Metabolic and Molecular Bases of Inherited Disease*. C. R. Scriver, A. L. Beaudet, W. S. Sly, and D. Valle, editors. McGraw-Hill Book Co., New York. 1933-1951.
8. Carlson, L. A., and B. Philipson. 1979. Fish-eye disease. New familial condition with massive corneal opacities and dyslipoproteinemia. *Lancet.* **ii**: 921-924.
9. Assmann, G., A. Von Eckardstein, and H. B. Brewer. 1995. Familial high density lipoprotein deficiency. In *The Metabolic and Molecular Bases of Inherited Disease*. C. R. Scriver, A. L. Beaudet, W. S. Sly, and D. Valle, editors. McGraw-Hill Book Co., New York. 2053-2072.
10. Schindler, P. A., C. Settiner, X. Collet, C. J. Fielding, and A. L. Burlingame. 1995. Site-specific detection and structural characterization of the glycosylation of human plasma proteins lecithin:cholesterol acyltransferase and apolipoprotein D using HPLC/electrospray mass spectrometry and sequential glycosidase detection. *Protein Sci.* **4**: 791-803.
11. Jauhiainen, M., and P. J. Dolphin. 1986. Human plasma lecithin:cholesterol acyltransferase. An elucidation of the catalytic mechanism. *J. Biol. Chem.* **261**: 7032-7043.
12. Francone, O. L., and C. J. Fielding. 1991. Structure-function relationships of human lecithin cholesterol acyltransferase. Site directed mutagenesis at serine residues 181 and 216. *Biochemistry.* **30**: 10074-10077.
13. Peelman, F., N. Vinaimont, A. Verhee, B. Vanloo, J. L. Verschelde, C. Labeur, S. Séguret-Macé, N. Duverger, G. Hutchinson, J. Vandekerckhove, J. Tavernier, and M. Rosseneu. 1998. Proposed architecture for lecithin:cholesterol acyltransferase. Identification of the catalytic triad and molecular modeling of LCAT. *Protein Sci.* **7**: 587-599.
14. Blanco-Vaca, F., S. J. Qu, C. Fiol, H. Z. Fan, Q. Pao, C. A. Marzal, J. J. Albers, I. Hurtado, V. Gracia, X. Pinto, T. Marti, and H. J. Pownall. 1997. Molecular basis of fish-eye disease in a patient from Spain. Characterization of a novel mutation in the LCAT gene and lipid analysis of the cornea. *Arterioscler. Thromb. Vasc. Biol.* **17**: 1382-1391.
15. Duverger N., H. Klein, G. Luc, J. Fruchart, J. Albers, H. Brewer, and S. Santamarina-Fojo. 1993. Identification of a novel mutation in the LCAT gene resulting in fish eye disease with  $\alpha$ -LCAT activity. *Circulation.* **88**: I-423 #2274. (Abstract).
16. Elkhailil L., Z. Majd, R. Bakir, O. Perez-Mendez, G. Castro, P. Poulain, B. Lacroix, N. Duhail, J. Fruchart, and G. Luc. 1997. Fish-eye disease: structural and in vivo metabolic abnormalities of high-density lipoproteins. *Metabolism.* **46**: 474-483.
17. Wilson, R., R. Ainscough, K. Anderson, C. Baynes, M. Berks, J. Bonfield, J. Burton, M. Connell, T. Copsey, and J. Cooper. 1994. 2.2 Mb of contiguous nucleotide sequence from chromosome III of *C. elegans*. *Nature.* **368**: 32-38.
18. Verhasselt, P., R. Aert, M. Vet, and G. Volckaert. 1994. Twelve open reading frames revealed in the 23.6 kb segment flanking the centromere on the *Saccharomyces cerevisiae* chromosome XIV right arm. *Yeast.* **10**: 1355-1361.
19. Thompson, J. D., D. G. Higgins, and T. J. Gibson. 1994. CLUSTAL W: improving the sensitivity of progressive multiple sequence alignment through sequence weighting, position-specific gap penalties and weight matrix choice. *Nucleic Acids Res.* **22**: 4673-4680.
20. Livingstone, C. D., and G. J. Barton. 1993. Protein sequence alignments: a strategy for the hierarchical analysis of residue conservation. *Comput. Appl. Biosci.* **9**: 745-756.
21. Barton, G. J. 1993: ALSCRIPT: a tool to format multiple sequence alignments. *Protein Eng.* **6**: 37-40.
22. Ollis, D. L., E. Cheah, M. Cygler, B. Dijkstra, F. Frolow, S. Franken, M. Harel, S. J. Remington, I. Silman, J. Schrag, J. L. Sussman, K. H. G. Verschueren, and A. Goldman. 1992. The  $\alpha/\beta$  hydrolase fold. *Protein Eng.* **5**: 197-211.
23. Winkler, F. K., A. d'Arcy, and W. Hunziker. 1990. Structure of human pancreatic lipase. *Nature.* **343**: 771-774.
24. Hide, W. A., L. Chan, and W. H. Li. 1992. Structure and evolution of the lipase superfamily. *J. Lipid Res.* **33**: 167-178.
25. Wang, J. C., A. K. Gebre, R. A. Anderson, and J. S. Parks. 1997. Amino acid residue 149 of lecithin:cholesterol acyltransferase determines phospholipase A(2) and transacylase fatty acyl specificity. *J. Biol. Chem.* **272**: 280-286.
26. Francone, O., L. Evangelista, and C. Fielding. 1996. Effects of carboxy-terminal truncation on human lecithin:cholesterol acyltransferase activity. *J. Lipid Res.* **37**: 1609-1615.
27. McLean, J. 1992. Molecular defects in the lecithin:cholesterol acyltransferase gene. In *High Density Lipoproteins and Atherosclerosis III*. N. E. Miller and A. Tall, editors. Excerpta Medica, Amsterdam. 59-65.
28. Funke, H., A. von Eckardstein, P. H. Pritchard, A. E. Hornby, H. Wiebusch, C. Motti, M. R. Hayden, C. Datchet, B. Jacotot, U. Gerdes, O. Faergeman, J. J. Albers, N. Colleoni, A. Catapano, J. Frohlich, G. Assmann, M. Kleingunnewigk, and A. Reckwerth. 1993. Genetic and phenotypic heterogeneity in familial lecithin:cholesterol acyltransferase (LCAT) deficiency—6 newly identified defective alleles further contribute to the structural heterogeneity in this disease. *J. Clin. Invest.* **91**: 677-683.
29. Guérin, M., P. J. Dolphin, and M. J. Chapman. 1993. Familial lecithin:cholesterol acyltransferase deficiency: further resolution of lipoprotein particle heterogeneity in the low density interval. *Atherosclerosis.* **104**: 195-212.
30. Dorval, I., P. Jezequel, C. Dubourg, B. Chauvel, P. Le Pogamp, and J. Le Gall. 1994. Identification of the homozygous missense mutation in the lecithin:cholesterol-acyltransferase (LCAT) gene, causing LCAT familial deficiency in two French patients. *Atherosclerosis.* **105**: 251-252.
31. Hill, J. S. 1994. The molecular pathology of lecithin:cholesterol acyltransferase deficiency. PHD Dissertation.
32. Qu, S. J., H. Z. Fan, F. Blanco-Vaca, and H. J. Pownall. 1995. In vitro expression of natural mutants of human lecithin:cholesterol acyltransferase. *J. Lipid Res.* **36**: 967-974.
33. Moriyama, K., J. Sasaki, F. Arakawa, N. Takami, E. Maeda, A. Matsunaga, Y. Takada, K. Midorikawa, T. Yanase, G. Yoshino, S. M. Marcovina, J. J. Albers, and K. Arakawa. 1995. Two novel point mutations in the lecithin:cholesterol acyltransferase (LCAT) gene resulting in LCAT deficiency: LCAT (G<sup>873</sup> deletion) and LCAT (Gly<sup>344</sup>→Ser). *J. Lipid. Res.* **36**: 2329-2343.
34. Klein, H. G., P. Lohse, P. H. Pritchard, D. Bojanovski, H. Schmidt, and H. B. Brewer, Jr. 1992. Two different allelic mutations in the lecithin:cholesterol acyltransferase gene associated with the fish eye syndrome. Lecithin:cholesterol acyltransferase (Thr123→Ile) and lecithin:cholesterol acyltransferase (Thr347→Met). *J. Clin. Invest.* **89**: 499-506.
35. Klein, H. G., N. Duverger, J. J. Albers, S. Marcovina, H. B. Brewer, and S. Santamarina-Fojo. 1995. In vitro expression of structural de-

- fects in the lecithin:cholesterol acyltransferase gene. *J. Biol. Chem.* **270**: 9443–9447.
36. Yang, X., A. Inazu, A. Honjo, I. Koizumi, K. Kajinami, J. Koizumi, S. Marcovina, J. Albers, and H. Mabuchi. 1997. Catalytically inactive lecithin:cholesterol acyltransferase (LCAT) caused by a Gly 30 to Ser mutation in a family with LCAT deficiency. *J. Lipid Res.* **38**: 585–591.
  37. Wiebusch, H., P. Cullen, J. S. Owen, D. Collins, P. S. Sharp, H. Funke, and G. Assmann. 1995. Deficiency of lecithin:cholesterol acyltransferase due to compound heterozygosity of two novel mutations (Gly33Arg and 30 bp ins) in the LCAT gene. *Hum. Mol. Genet.* **4**: 143–145.
  38. Jauhainen, M., K. J. Stevenson, and P. J. Dolphin. 1988. Human plasma lecithin:cholesterol acyltransferase. The vicinal nature of cysteine 31 and cysteine 184 in the catalytic site. *J. Biol. Chem.* **263**: 6525–6533.
  39. Taramelli, R., M. Pontoglio, G. Candiani, S. Ottolenghi, H. Dieplinger, A. Catapano, J. Albers, C. Vergani, and J. McLean. 1990. Lecithin:cholesterol acyltransferase deficiency: molecular analysis of a mutated allele. *Hum. Genet.* **85**: 195–199.
  40. Klein, H. G., P. Lohse, N. Duverger, J. J. Albers, D. J. Rader, L. A. Zech, S. Santamarina-Fojo, and H. B. Brewer, Jr. 1993. Two different allelic mutations in the lecithin:cholesterol acyltransferase (LCAT) gene resulting in classic LCAT deficiency: LCAT (tyr<sup>83</sup>→stop) and LCAT (tyr<sup>156</sup>→asn). *J. Lipid Res.* **34**: 49–58.
  41. Peelman, F., Goethals, M. Vanloo, B. Brasseur, R. Vandekerckhove, J. and M. Rosseneu. 1997. Structural and functional properties of WT and variant peptides of the 154–171 segment of lecithin:cholesterol acyltransferase. *Eur. J. Biochem.* **249**: 708–715.
  42. Hill, J. S., X. Wang, and P. H. Pritchard. 1993. Lecithin:cholesterol acyltransferase deficiency: identification of a causative gene mutation and a co-inherited protein polymorphism. *Biochim. Biophys. Acta.* **1181**: 321–323.
  43. Kuivenhoven, J. A., A. F. H. Stalenhoef, J. S. Hill, P. N. M. Demacker, A. Errami, J. J. P. Kastelein, and P. H. Pritchard. 1996. Two novel molecular defects in the LCAT gene are associated with fish eye disease. *Arterioscler. Thromb. Vasc. Biol.* **16**: 294–303.
  44. Steyrer, E., S. Haubenwallner, G. Horl, W. Giessauf, G. M. Kostner, and R. Zechner. 1995. A single G to A nucleotide transition in exon IV of the lecithin:cholesterol acyltransferase (LCAT) gene results in an Arg140 to His substitution and causes LCAT deficiency. *Hum. Genet.* **96**: 105–109.
  45. Funke, H., A. Von Eckardstein, P. H. Pritchard, J. J. Albers, J. J. P. Kastelein, C. Drought, and G. Assmann. 1991. A molecular defect causing fish eye disease: an amino acid exchange in lecithin:cholesterol acyltransferase (LCAT) leads to the selective loss of alpha-LCAT activity. *Proc. Natl. Acad. Sci. USA.* **88**: 413–419.
  46. Contacos, C., D. R. Sullivan, K-A. Rye, H. Funke, and G. Assmann. 1996. A new molecular defect in the lecithin:cholesterol acyltransferase (LCAT) gene associated with fish eye disease. *J. Lipid Res.* **37**: 35–44.
  47. O, K., J. S. Hill, X. Wang, and P. H. Pritchard. 1993. Recombinant lecithin:cholesterol acyltransferase containing a Thr<sup>123</sup>→Ile mutation esterifies cholesterol in low density lipoprotein but not in high density lipoprotein. *J. Lipid Res.* **34**: 81–88.
  48. Kuivenhoven, J. A., E. J. van Voorst tot Voorst, H. Wiebusch, S. M. Marcovina, H. Funke, G. Assmann, P. H. Pritchard, and J. J. Kastelein. 1995. A unique genetic and biochemical presentation of fish-eye disease. *J. Clin. Invest.* **96**: 2783–2791.
  49. Frohlich, J., G. R. Hoag, M. McLeod, D. V. Hayden, L. D. Godin, J. D. Wadworth, S. Crichley, and P. H. Pritchard. 1987. Hypoalphalipoproteinemia resembling fish eye disease. *Acta Med. Scand.* **221**: 291–298.
  50. Skretting, G., J. P. Blomhoff, J. Solheim, and H. Prydz. 1992. The genetic defect of the original Norwegian lecithin:cholesterol acyltransferase deficiency families. *FEBS Lett.* **309**: 307–310.
  51. Skretting, G., and H. Prydz. 1992. An amino acid exchange in exon I of the human lecithin:cholesterol acyltransferase (LCAT) gene is associated with fish eye disease. *Biochem. Biophys. Res. Commun.* **182**: 583–587.
  52. Klein, H. G., S. Santamarina-Fojo, N. Duverger, M. Clerc, M. F. Dumon, J. J. Albers, S. Marcovina, and H. B. Brewer. 1993. Fish eye syndrome—a molecular defect in the lecithin:cholesterol acyltransferase (LCAT) gene associated with normal alpha-LCAT-specific activity—implications for classification and prognosis. *J. Clin. Invest.* **92**: 479–485.
  53. Derewenda, Z. S., and C. Cambillau. 1991. Effects of gene mutations in lipoprotein and hepatic lipases as interpreted by a molecular model of the pancreatic triglyceride lipase. *J. Biol. Chem.* **266**: 23112–23119.